IOP Publishing and International Atomic Energy Agency — Nuclear Fusion
Nucl. Fusion 49 (2009) 065019 (7pp) doi:10.1088/0029-5515/49/6/065019

Relaxed MHD states of a multiple region plasma

M.J. Hole[a], R. Mills, S. R. Hudson[1] and R.L. Dewar

Research School of Physics and Engineering, Australian National University, ACT 0200, Australia
[1] Princeton Plasma Physics Laboratory, PO Box 451, Princeton, NJ 08543, USA

E-mail: matthew.hole@anu.edu.au

Received 12 January 2009, accepted for publication 20 April 2009
Published 19 May 2009
Online at stacks.iop.org/NF/49/065019

Abstract
We calculate the stability of a multiple relaxation region MHD (MRXMHD) plasma, or stepped-Beltrami plasma, using both variational and tearing mode treatments. The configuration studied is a periodic cylinder. In the variational treatment, the problem reduces to an eigenvalue problem for the interface displacements. For the tearing mode treatment, analytic expressions for the tearing mode stability parameter Δ', being the jump in the logarithmic derivative in the helical flux across the resonant surface, are found. The stability of these treatments is compared for $m = 1$ displacements of an illustrative reverse field pinch-like configuration, comprising two distinct plasma regions. For pressureless configurations, we find the marginal stability conclusions of each treatment to be identical, confirming the analytical results in the literature. The tearing mode treatment also resolves ideal MHD unstable solutions for which $\Delta' \to \infty$: these correspond to displacement of a resonant interface. Wall stabilization scans resolve the internal and external ideal kink. Scans with increasing pressure are also performed: these indicate that both variational and tearing mode treatments have the same stability trends with β, and show destabilization in configurations with increasing core pressure. Combined, our results suggest that variational stability of MRXMHD configurations is sufficient for both ideal and tearing ($\Delta' < 0$) stability. Such configurations, and their stability properties, are of emerging importance in the quest to find mathematically rigorous solutions of ideal MHD force balance in 3D geometry.

PACS numbers: 52.35.Bj, 52.35.Py, 52.55.−s, 52.55.Hc, 52.55.Lf, 52.55.Tn

1. Introduction

Recently, Hole *et al* [1] proposed a model for a partially relaxed plasma–vacuum system. The purpose of the model, which abandons all but a small number of flux surfaces, is to provide a mathematically rigorous foundation for MHD equilibria in 3D configurations. The model is based on a generalization of the Taylor relaxation model in which the total energy (field plus plasma) is minimized subject to a finite number of magnetic flux, helicity and thermodynamic constraints. These constraints apply to relaxation regions in which the plasma behaves as an ideal gas confined by toroidal barrier interfaces, which are arbitrarily thin, deformable ideal MHD regions. The relaxation can be due to any mechanism that breaks magnetic confinement and thus includes tearing and field-line chaos. The model thus leads to a stepped pressure profile, with the pressure jumps across the barrier interfaces being counterbalanced by corresponding magnetic field jumps, which may or may not include jumps in rotational transform. Our overarching objective is the development of an equilibrium solver for 3D plasmas built on a closely spaced stepped pressure profile model.

In the 3D case, we envisage that the barriers can be chosen to be nonresonant KAM surfaces that survive the onset of field-line chaos intrinsic to 3D equilibria. In between these interfaces, the field is Beltrami, such that $\nabla \times \boldsymbol{B} = \mu \boldsymbol{B}$, with μ a constant. The boundary condition across the interfaces is the continuity of total pressure $P + B^2/(2\mu_0)$. Such a model, which we term a multiple relaxation region MHD (MRXMHD) model, raises a number of questions. How should the equilibrium be constrained? How much jump in pressure and/or rotational transform $\iota\!\!\!-$ can each interface support? Are the interfaces stable to deformation? Can the class of stability shed information onto other quasi-relaxed phenomena?

Previous work has focused on the equilibrium constraints [2, 3], construction of a numerical algorithm for calculation of Beltrami fields between interfaces in 3D configurations [4] and a variational principle for the equilibrium and stability of the multiple interface configuration in cylindrical plasmas [1].

[a] Author to whom any correspondence should be addressed.

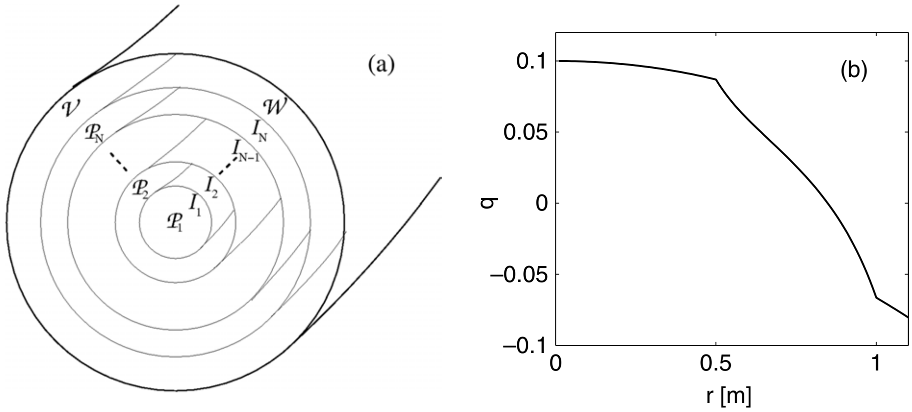

Figure 1. Schematic of magnetic geometry (*a*), showing ideal MHD barriers $\mathcal{I}_i$, the conducting wall $\mathcal{W}$, plasma regions $\mathcal{P}_i$ and the vacuum $\mathcal{V}$. Panel (*b*) shows the q profile used for stability studies in section 4, with $\mu_1 = 2$ (core) and $\mu_2 = 3.6$ (edge).

We have also explored the relationship between relaxed plasma equilibrium models discussed here, and entropy related plasma self-organization principles [5].

This work, which studies the tearing mode stability of 2D configurations, and compares and contrasts stability conclusions with those of the MRXMHD variational principle, complements a separate publication [6] that unifies relaxed and ideal MHD principles for constructing global solutions comprising mixed relaxed and ideal regions. To conduct a comparative study, we have selected perturbations with a particular poloidal mode number, $m = 1$. While it was not our intent to study the comprehensive stability of the plasma for all Fourier modes, there is value in elucidating the relevance of the results to modes with $m \neq 1$. In Mills [6], we have shown that the linear displacement perturbation ξ obeys the same Euler–Lagrange equation of Newcomb [7] for both relaxed and ideal MHD perturbation, except in the neighbourhood of the magnetic surfaces where $\boldsymbol{B}\cdot\nabla$ is singular. In cylindrical geometry, the difference between treatments lies in the class of solutions allowed: in ideal MHD only Newcomb's small solutions are allowed, whereas in relaxed MHD only the odd-parity large solution and even-parity small solution are allowed. Given ξ obeys the same Euler–Lagrange equation, we utilize the proof of Newcomb that to demonstrate a configuration is stable, it is sufficient to show that it is stable for all values of the axial wavenumber κ when $m = 1$ and for $m = 0, \kappa \to 0$. The latter class, $m = 0, \kappa \to 0$, corresponds to a change of equilibrium state. We assume that we have chosen the 'lowest' equilibrium state, such that $m = 0, \kappa \to 0$ modes are stable.

A second motivation for this work is to extend a recent tearing mode stability treatment developed for a zero pressure, no-vacuum, reverse field pinch (RFP) [8], to more realistic plasma configurations, by including nonzero pressure and a vacuum region. Recently, Tassi *et al* [8], performed a tearing mode stability treatment on stepped μ force-free equilibria close to Taylor-relaxed states. The purpose of their work was to develop a mechanism for the formation of cyclic Quasi-single-helicity (QSH) states observed in RFPs [9]. They consider a cylindrical plasma divided into two different Beltrami regions, and encased in a perfectly conducting shell, and compute the tearing mode stability parameter Δ' at a resonant radius r_s for a helical flux perturbation $\chi_1(r) = mB_{z1}(r) - \kappa r B_{\theta 1}(r)$. Here r is the radial coordinate and m and κ the poloidal and axial wave number. Tassi *et al* [8] find critical values of the jump in μ, beyond which the RFP-like plasma is unstable. Based on these, they postulate the QSH state may be viewed as a small, cyclic departure from a Taylor-relaxed state.

We extend the tearing mode stability treatment of Tassi *et al* [8] to plasmas with finite pressure and a vacuum region, and compare stability conclusions of our variational treatment to that of a tearing mode stability analysis. Our paper is arranged as follows: section 2 summarizes the variational model of stepped pressure profile plasmas, presented in Hole *et al* [1], and introduces a tearing mode model. Section 3 treats MRXMHD plasmas in cylindrical geometry, yielding stability parameter expressions for both the variational and tearing mode treatments. In section 4, we compute $m = 1$ stability for an example configuration, draw comparisons between the stability conclusions based on variational and tearing mode treatments, and explore marginal stability limits in wavenumber space as a function of pressure. Finally, section 5 contains concluding remarks.

2. Multiple interface plasma–vacuum model

The system comprises N Taylor-relaxed plasma regions, each separated by an ideal MHD barrier. The outermost plasma region is enclosed by a vacuum, and encased in a perfectly conducting wall. Figure 1(*a*) shows the geometry of the system, and introduces the nomenclature used to describe the region and interfaces. The regions $\mathcal{R}_i$ comprise the N plasma regions $\mathcal{R}_1 = \mathcal{P}_1, \ldots, \mathcal{R}_N = \mathcal{P}_N$ and the vacuum region $\mathcal{R}_{N+1} = \mathcal{V}$. Each plasma region $\mathcal{P}_i$ is bounded by the inner and outer ideal MHD interfaces $\mathcal{I}_{i-1}$ and $\mathcal{I}_i$ respectively, whilst the vacuum is encased by the perfectly conducting wall $\mathcal{W}$.

2.1. A variational description

In previous work [1] we outlined our variational principle, which lies between that of Kruskal and Kulsrud [10]—minimization of total energy $W \equiv \int [B^2/(2\mu_0) + P/(\gamma - 1)]\mathrm{d}\tau$ (where P is plasma pressure, γ the ratio of specific heats, and $\mathrm{d}\tau$ a volume element) under the uncountable infinity of constraints provided by applying ideal MHD within each fluid element—and the relaxed MHD of Woltjer [11] and Taylor

[12]—minimization of W holding only the two global toroidal and poloidal magnetic fluxes, and the single global ideal MHD helicity invariant $H \equiv \int \boldsymbol{A}\cdot\boldsymbol{B}$, constant. In summary, the energy functional could be written

$$W = \sum_{i=1}^{N} U_i - \sum_{i=1}^{N} \mu_i H_i/2 - \sum_{i=1}^{N} \nu_i M_i, \tag{1}$$

where μ_i and ν_i are Lagrange multipliers and

$$U_i = \int_{\mathcal{R}_i} \mathrm{d}\tau \left(\frac{P}{\gamma - 1} + \frac{B^2}{2\mu_0} \right), \tag{2}$$

$$M_i = \int_{\mathcal{R}_i} \mathrm{d}\tau\, P^{1/\gamma}, \tag{3}$$

$$H_i = \int_{\mathcal{R}_i} \mathrm{d}\tau \boldsymbol{A}\cdot\nabla\times\boldsymbol{A} + \oint_{C^{<}_{p,i}} \mathbf{d}\boldsymbol{l}\cdot\boldsymbol{A} \oint_{C^{<}_{t,i}} \mathbf{d}\boldsymbol{l}\cdot\boldsymbol{A} - \oint_{C^{>}_{p,i}} \mathbf{d}\boldsymbol{l}\cdot\boldsymbol{A} \oint_{C^{>}_{t,i}} \mathbf{d}\boldsymbol{l}\cdot\boldsymbol{A}. \tag{4}$$

The term U_i is the potential energy, M_i the plasma mass and H_i the magnetic helicity in each region $\mathcal{R}_i$. In equations (2)–(4), P is the equilibrium pressure, B the field strength and $\boldsymbol{A}$ the vector potential. The superscripts $^{>}$ and $^{<}$ denote rotations about the magnetic field on the inner and outer boundaries of the regions $\mathcal{R}_i$, respectively.

Setting the first variation to zero yields the following set of equations:

$$\mathcal{P}_i;\ \nabla\times\boldsymbol{B} = \mu_i\boldsymbol{B}, \qquad P_i = \text{const.}, \tag{5}$$

$$\mathcal{I}_i;\ \boldsymbol{n}\cdot\boldsymbol{B} = 0, \qquad [[P_i + B^2/(2\mu_0)]] = 0, \tag{6}$$

$$\mathcal{V};\ \nabla\times\boldsymbol{B} = 0, \qquad \nabla\cdot\boldsymbol{B} = 0, \tag{7}$$

$$\mathcal{W};\ \boldsymbol{n}\cdot\boldsymbol{B} = 0, \tag{8}$$

where $\boldsymbol{n}$ is a unit vector normal to the plasma interface $\mathcal{I}_i$ and $[[x]] = x_{i+1} - x_i$ denotes the change in quantity x across the interface $\mathcal{I}_i$. The boundary conditions, $\boldsymbol{n}\cdot\boldsymbol{B} = 0$, arise because each interface and the conducting wall is assumed to have infinite conductivity. In turn, these imply the toroidal flux in each plasma region (and the poloidal flux in the vacuum) is constant during relaxation. Given the vessel with boundary $\mathcal{W}$, the interfaces $\mathcal{I}_i$ and the magnetic field $\boldsymbol{B}$, equations (5)–(8) constitute a boundary problem for the plasma pressure P_i in each region $\mathcal{R}_i$. If the properties of the plasma are prescribed on the interface, equation (5) becomes a nonlinear eigenvalue problem for the Lagrange multipliers, μ_i, which has an infinite number of discrete solutions. Different solutions correspond to a different number of poles in the rotational transform [4].

Minimizing the second variation subject to the constraint of the positive definite normalization $\sum_i^N \int_{\mathcal{I}_i} \mathrm{d}\sigma |\xi_i|^2$, with $d\sigma$ an area element on $\mathcal{I}_i$, yields the following set of equations for the variation in the magnetic field $\boldsymbol{b} = \delta\boldsymbol{B}$:

$$\mathcal{P}_i;\ \nabla\times\boldsymbol{b} = \mu_i\boldsymbol{b}, \tag{9}$$

$$\mathcal{I}_i;\ \xi_i^*[[\boldsymbol{B}\cdot\boldsymbol{b}]] + \xi_i^*\xi_i[[B(\boldsymbol{n}\cdot\nabla)B]] - \lambda\xi_i^*\xi_i = 0, \tag{10}$$

$$\boldsymbol{n}\cdot\boldsymbol{b}_{i,i+1} = \boldsymbol{B}_{i,i+1}\cdot\nabla\xi_i + \xi_i\boldsymbol{n}\cdot\nabla\times(\boldsymbol{n}\times\boldsymbol{B}_{i,i+1}), \tag{11}$$

$$\mathcal{V};\ \nabla\times\boldsymbol{b} = 0, \qquad \nabla\cdot\boldsymbol{b} = 0, \tag{12}$$

$$\mathcal{W};\ \boldsymbol{n}\cdot\boldsymbol{b} = 0. \tag{13}$$

Here $\boldsymbol{\xi}_i$ is the normal displacement of the interface I_i and λ is the Lagrange multiplier of the stability treatment, such that $\lambda < 0$ indicates a lower energy state is available. Using equations (9)–(13) the perturbed flux through each region can be found. With a suitable Fourier decomposition chosen, equation (11) solves for the unknown coefficients of the perturbed field in each region. With substitution, equation (10) then becomes a linear eigenvalue equation for λ.

2.2. *Tearing mode treatment*

A starting point for the treatment of tearing modes is the set of MHD equations:

$$\frac{\partial\rho}{\partial t} + \nabla\cdot\rho\boldsymbol{v} = 0, \tag{14}$$

$$\rho\frac{\mathrm{d}\boldsymbol{v}}{\mathrm{d}t} = \boldsymbol{J}\times\boldsymbol{B} - \nabla p, \tag{15}$$

$$\frac{\mathrm{d}}{\mathrm{d}t}\frac{p}{\rho^{\gamma_{\text{gas}}}} = 0, \tag{16}$$

$$\boldsymbol{E} + \boldsymbol{v}\times\boldsymbol{B} = \eta\boldsymbol{J}, \tag{17}$$

$$\nabla\times\boldsymbol{E} = -\partial\boldsymbol{B}/\partial t, \tag{18}$$

$$\nabla\times\boldsymbol{B} = \mu_0\boldsymbol{J}, \tag{19}$$

$$\nabla\cdot\boldsymbol{B} = 0, \tag{20}$$

being mass continuity, the fluid equation of motion, the adiabatic equation of state, Ohm's law, Faraday's law, Ampere's law and magnetic monopole condition, respectively. Here $\boldsymbol{v}$ is the fluid velocity, ρ is the plasma mass density, $\boldsymbol{J}$ is the current density, η is the plasma resistivity and t is the time. The plasma parameters change across each interface and across surfaces with resonant perturbations (i.e. perturbations which satisfy $\boldsymbol{\kappa}\cdot B = 0$, with $\boldsymbol{\kappa}$ the wave vector of the perturbation).

We solve for the plasma parameters for a zero flow plasma (i.e. $\boldsymbol{v} = 0$) in 'outer' regions away from the resonant surfaces where the effects of resistivity are negligible. To solve, the field is written $\boldsymbol{B} = \nabla\chi\times\boldsymbol{h} + g\boldsymbol{h}$, where g and χ are scalar functions of position and time and $\boldsymbol{h}$ is the helical field vector. Next, χ and g are expanded as a Fourier perturbation, and solutions to the linearized Beltrami equation are found. The ODE for $\chi_1(r)$, the radial envelope of the linear Fourier perturbation for χ, integrates to a jump condition in $\chi_1(r)'/\chi_1(r)$ at each interface, expressed in terms of equilibrium parameters. The perturbation growth rate, obtained by linearizing Faraday's law and substituting for $\boldsymbol{E}$ as determined by Ohm's law, is proportional to

$$\Delta' = \left[\chi_1(r)'/\chi_1(r)\right]_{r_s^-}^{r_s^+}, \tag{21}$$

such that $\Delta' = 0$ denotes marginal stability and $\Delta' > 0$ instability. Here r_s is the radial position of the resonant surface and $r_s^{\pm} = r_s + 0^{\pm}$. The final expression for Δ' is a function of the equilibrium parameters in the resonant region, as well as jumps in equilibrium parameters across the interfaces.

3. MRXMHD cylindrical plasmas

Equilibrium solutions in an azimuthally and axially symmetric cylinder are available in Hole *et al* [1]. In the cylindrical coordinate system (r, θ, z) they are

$$\begin{aligned} &\mathcal{P}_1 : \boldsymbol{B} = \{0, \quad k_1 J_1(\mu_1 r), \quad k_1 J_0(\mu_1 r)\},\\ &\mathcal{P}_i : \boldsymbol{B} = \big\{0, \quad k_i J_1(\mu_i r) + d_i Y_1(\mu_i r),\\ &\quad k_i J_0(\mu_i r) + d_i Y_0(\mu_i r)\big\},\\ &\mathcal{V} : \boldsymbol{B} = \{0, \quad B_\theta^V/r, \quad B_z^V\}, \end{aligned} \tag{22}$$

where $k_i, d_i \in \Re$ and J_0, J_1 and Y_0, Y_1 are Bessel functions of the first kind of order 0, 1, and second kind of order 0, 1, respectively. The terms B_θ^V and B_z^V are constants. The constant d_1 is zero in the plasma core $\mathcal{P}_1$, because the Bessel functions $Y_0(\mu_1 r)$ and $Y_1(\mu_1 r)$ have a simple pole at $r = 0$. Radius is normalized to the plasma–vacuum boundary, located at $r = 1$. The equilibrium is constrained by the $4N + 1$ parameters:

$$\{k_1, ..., k_N, d_2, ..., d_N, \mu_1, ..., \mu_N, r_1, ...r_{N-1}, r_{\rm w}, B_\theta^V, B_z^V\}, \tag{23}$$

where r_i are the radial positions of the N ideal MHD barriers, $r_N = 1$ and $r_{\rm w}$ is the radial position of the conducting wall. Equivalent representations and the mapping between these solutions has been discussed in earlier work [2].

3.1. Stability from a variational principle

We have assessed stability using a Fourier decomposition in the poloidal and axial directions for the perturbed field $\boldsymbol{b} = \nabla \times \boldsymbol{a}$ and the displacements ξ_i of each interface. That is,

$$\boldsymbol{b} = \widetilde{\boldsymbol{b}} e^{i(m\theta+\kappa z)}, \xi_i = X_i e^{i(m\theta+\kappa z)}, \tag{24}$$

where m, κ are the Fourier poloidal mode number and axial wave number and $\widetilde{\boldsymbol{b}}/\boldsymbol{b}$ and X_i are complex Fourier amplitudes. Under these substitutions, and after solving for the field in each region, equation (10) reduces to an eigenvalue matrix equation $\boldsymbol{\eta} \cdot \boldsymbol{X} = \lambda \boldsymbol{X}$ with column eigenvector $\boldsymbol{X} = (\xi_1, \ldots, \xi_N)^T$, eigenvalue λ, and $\boldsymbol{\eta}$ a $N \times N$ tridiagonal real matrix.

3.2. Tearing mode stability

In the helical coordinate $u = m\theta + \kappa z$, a divergence-less $\boldsymbol{B}$ can be written

$$\boldsymbol{B}(r, u) = \nabla\chi(r, u) \times \boldsymbol{h} + g(r, u)\boldsymbol{h}, \tag{25}$$

where χ is a helical flux, and $g\boldsymbol{h}$ a helical field. The vector $\boldsymbol{h}$ is defined by $\boldsymbol{h} = f(r)\nabla r \times \nabla u$, where $f(r) = r/(m^2+\kappa^2 r^2)$ is a metric term. As in Tassi *et al* [8] we search for helical perturbations of the form

$$\begin{aligned} \chi(r, u, t) &= \chi_0(r) + \chi_1(r) e^{\gamma t + iu},\\ g(r, u, t) &= g_0(r) + g_1(r) e^{\gamma t + iu}. \end{aligned} \tag{26}$$

In this representation, resonant surfaces are those for which $\chi_0'(r) = 0$. The equilibrium field satisfies the Beltrami equation, giving rise to $\mu = g_0'(r)/\chi_0'(r)$, such that the rotational transform can be written

$$\iota = -\frac{R}{r} \times \frac{r\kappa g_0(r)/\chi_0'(r) + m}{m g_0(r)/\chi_0'(r) - r\kappa}. \tag{27}$$

Here we have elected to make all plasma perturbations axially periodic, with axial periodicity length $L = 2\pi R$, such that r/R is an effective inverse aspect ratio of the plasma. This assumption discretizes the wavenumber such that $\kappa = -n/R$, where n takes the set of integers. We adopt this change of notation in section 4.

By writing the incompressible velocity field in a similar form to equation (25), and expanding continuity to first order, it is possible to show perturbations in the flow, pressure and mass density do not affect marginal stability. In each of the plasma regions, projections of the linearized Beltrami equation along $\boldsymbol{h}$ and ∇r yield

$$g_1 = g_0'(r)/\chi_0'(r)\chi_1(r), \tag{28}$$

$$\chi_0(r)\left[\chi_1''(r) + \frac{f'(r)}{f(r)}\chi_1'(r) + \left(\mu^2 - \frac{1}{rf(r)} + \frac{g_0(r)}{\chi_0'(r)}\mu' + \frac{2m\kappa}{m^2+\kappa^2 r^2}\mu\right)\chi_1(r)\right] = 0, \tag{29}$$

where μ' vanishes everywhere except at interface locations, where it becomes singular. These are identical to equations (27) and (29) of Tassi *et al* [8]. Under the transformation $x_i = r\sqrt{|\mu_i^2 - \kappa^2|}$, equation (29) reduces to a Bessel equation if $\kappa^2 < \mu^2$, or modified Bessel equation if $\kappa^2 \geqslant \mu^2$. In the vacuum region, and under the transformation $x_{N+1} = |\kappa|r$, equation (29) reduces to a modified Bessel equation. In the ith region, either side of the resonant surface, and in the vacuum, solutions are different combinations of Bessel or modified Bessel functions with undetermined coefficients $\zeta_i, \Lambda_i, \zeta_{i-s}, \Lambda_{i-s}, \zeta_{i+s}, \Lambda_{i+s}$, and ζ_V, Λ_V, respectively. As only the ratio $\chi_1'(r)/\chi_1(r)$ appears in Δ', its value is unaffected by normalizing $\zeta = 1$ in each interval and region. The requirement of boundedness at $r = 0$, and the presence of perfectly conducting wall implies

$$\chi_1(0) = \chi_0, \qquad \chi_1(r_w) = 0. \tag{30}$$

Noting that the perturbed flux must be continuous across each interface, equation (29) can then be integrated about each interface to yield

$$\left[\left[\chi_0'(r)\frac{\chi_1'(r)}{\chi_1(r)}\right]\right] = \left[\left[-\chi_0'(r)\frac{g_0(r)}{\chi_0'(r)}\mu\right]\right]. \tag{31}$$

The parametric dependence can also be examined by solving for $\chi_0(r)$ and using equation (27) to eliminate $g_0(r)/\chi_0'(r)$. Solving equilibrium for $\chi_0(r)$ gives

$$\chi_0'(r) = B\sqrt{\frac{m^2+\kappa^2 r^2}{\left(\dfrac{-mR/r + \kappa R\iota r/R}{\iota m + \kappa R}\right)^2 + 1}} = F(B, r, R, m, \kappa). \tag{32}$$

Finally, eliminating $\chi_0'(r)$ and $g_0(r)/\chi_0'(r)$, equation (31) can then be rewritten

$$\left[\left[F(B, r, R, m, \kappa)x_i\frac{\chi_1'(x_i)}{\chi_1(x_i)}\right]\right] = [[G(B, \mu, \iota, r, R, m, \kappa)]], \tag{33}$$

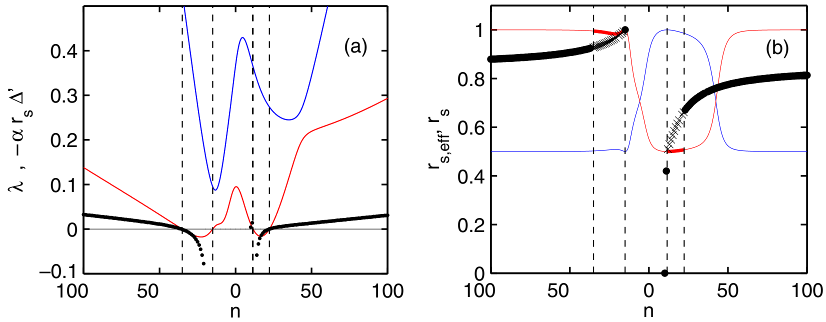

Figure 2. Dispersion curves (a) and mode localization (b) of $m = 1$ modes of a pressureless MRXMHD plasma with q profile given by figure 1(b). In panel (a), the solid lines are eigenvalues (λ) of the MRXMHD treatment, and represent different eigenfunctions, while the points are values of $-0.002 \times r_s\Delta'$ determined from tearing mode analysis of section 3.2. The vertical dashed lines correspond to zeros in λ. Panel (b) shows the resonant surfaces r_s of tearing modes (points), and effective localization $r_{s,\mathrm{eff}}$ of modes using the variational treatment (solid line). The solid points and cross-hairs denote stable and unstable tearing modes, respectively. The heavy solid line denotes solutions for which $\lambda < 0$, and the dashed vertical lines correspond to marginal stability, $\lambda = 0$.

(This figure is in colour only in the electronic version)

where the transformed variables $x_i = r\sqrt{|\mu_i^2 - \kappa^2|}$ are different in each region, and where

$$G(B, \mu, \iota\!\!\!-, r, R, m, \kappa) = r\mu F(B, r, R, m, \kappa) \times \frac{mR/r - \kappa R \iota\!\!\!- r/R}{\iota\!\!\!- m + \kappa R}. \qquad (34)$$

With $\zeta = 1$ everywhere, the tearing mode parameter $\Delta' = [\chi_1'(r)/\chi_1(r)]_{r_s^-}^{r_s^+}$ (see equation (21)) is a function of Λ either side of the resonant surface, and through equation (33), all Λ values. For example, suppose $\kappa^2 < \mu^2$ everywhere, and the resonant surface lies in the second Beltrami region. The general solution to equation (29) can then be written

$$\chi_1 = \begin{cases} \kappa x_1(J_{m-1}(x_1) - \Lambda_1 Y_{m-1}(x_1)) \\ \quad + m(\mu_1 - \kappa)(J_m(x_1) - \Lambda_1 Y_m(x_1)), & 0 < x_1 < x_{i1} \\ \kappa x_1(J_{m-1}(x_2) - \Lambda_{2-s} Y_{m-1}(x_2)) \\ \quad + m(\mu_1 - \kappa)(J_m(x_2) - \Lambda_{2-s} Y_m(x_2)), & x_{i1} < x_2 < x_s \\ \kappa x_2(J_{m-1}(x_2) - \Lambda_{2+s} Y_{m-1}(x_2)) \\ \quad + m(\mu_2 - \kappa)(J_m(x_1) - \Lambda_{2+s} Y_m(x_2)), & x_s < x_2 < x_{i2} \\ x_3(I_{m-1}(x_3) - \Lambda_V K_{m-1}(x_3)) \\ \quad + m(I_m(x_3) + \Lambda_V K_m(x_3)), & x_{i2} < x_3 < x_w \end{cases} \qquad (35)$$

where x_s is the value of x at the resonant surface, and where we have set $\zeta = 1$ everywhere. Using these solutions, the interface jump condition (equation (33)) at interface $\mathcal{I}_1$, can be solved for Λ_{2-s} in terms of Λ_1. Similarly, equation (33) at interface $\mathcal{I}_2$ can be solved for Λ_{2+s} in terms of Λ_V. Next, we apply the boundary conditions of equation (30) to equation (35). The function $Y_m(x_1)$ has a pole at $x_1 = 0$, and so $\chi_1(x_1) = 0$ requires $\Lambda_1 = 0$. Finally, using $\chi_1(r_w) = 0$, equation (35) can be solved for Λ_V. Thus, Λ_{2-s} and Λ_{2+s} are determined and Δ' can be evaluated.

Changes in the field strength B at any interface enter equation (31) through the solution to $\chi_0'(r)$, given by equation (32). Stability is hence a property of the rotational transform, the Lagrange multipliers, and any jumps in the pressure or rotational transform across the interfaces. If there are such jumps in pressure or rotational transform, stability is also a function of the position of the barriers. Our working reduces to Tassi *et al* [8] in the limit of no pressure, field or rotational transform jumps across the interfaces and no vacuum.

4. Stability for an RFP-like configuration

We have compared stability conclusions using variational and tearing mode treatments for an illustrative two-interface (i.e. $N = 2$) configuration. The example chosen is guided by earlier detailed working [1], where the core Lagrange multiplier was $\mu_1 = 2$. The internal interface is placed at $r_1 = 0.5$, the plasma–vacuum boundary positioned at $r_2 = 1$, and the axial periodicity length chosen to be 20π, such that the effective inverse aspect ratio $r_2/R = 1/10$ is small. The change in safety factor between the internal interface and the plasma–vacuum boundary has been chosen to resemble Hole *et al* [1], subject to the different R values used for the two treatments ($R = 1/(2\pi)$ in [1]). We have used $\mu_2 = 3.6$, which requires $d_2/k_2 = 0.77$ for the rotational transform profile to be continuous. A second motivation for this choice is the similarity to q profiles of high confinement RFPs, such as the Madison symmetric torus [13] and RFX-mod [14], although the change in μ is greatly exaggerated in this work. The plasma pressure is selected by the parametrization $\beta_1 = p_1/(B_V^2/2\mu_0)$, $\beta_2 = p_2/(B_V^2/2\mu_0)$. Except for the final scan over β, a pressureless plasma is assumed (i.e. $\beta_1 = \beta_2 = 0$). Figure 1(b) shows the q profile for the chosen equilibrium, where $q = 1/\iota\!\!\!-$.

Figure 2(a) is a dispersion curve for $m = 1$ modes, showing λ computed using the variational treatment, and $-r_s\Delta'$ computed for modes resonant within the plasma. Marginal stability corresponds to $\lambda = 0$ and $\Delta' = 0$: these overlap identically in figure 2(a). Modes with $n = -16$ and $n = 12$ correspond to perturbations near-resonant with the outer and inner interfaces ($q(r_2) \approx -1/16$ and $q(r_1) \approx 1/12$), respectively.

In our variational treatment, we have prescribed no relationship between ξ and $\boldsymbol{b}$ in the relaxed regions (see below for further discussion). As such, except on the ideal interfaces, field-line resonance in such plasmas is not explicitly resolved. Expressions can however be constructed which provide an estimate of the localization of the mode $r_{s,\mathrm{eff}}$, and a convenient choice is $r_{s,\mathrm{eff}}^2 = \sum_{i=1}^{N}(r_i X_i)^2$, where the eigenvectors are normalized such that $\boldsymbol{X} \cdot \boldsymbol{X}^H = 1$, with H the Hermitian.

Figure 2(b) shows a comparison of $r_{s,\mathrm{eff}}$ to r_s, in which modes unstable in the variational and tearing mode treatment

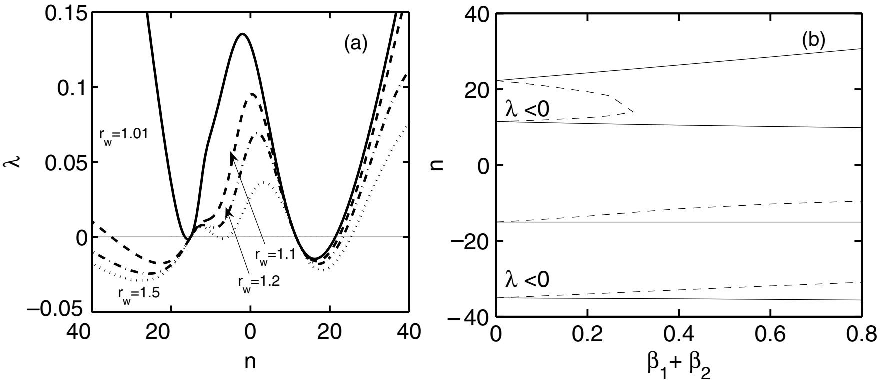

Figure 3. Wall stabilization (*a*) and marginal stability pressure dependence (*b*) of MRXMHD plasmas unstable to $m = 1$ modes. Panel (*a*) shows the dispersion curves of MRXMHD plasmas unstable to $m = 1$ modes as a function of n for different conducting wall radii. In panel (*b*) marginal stability $n - \beta$ space is shown for different pressure profile configurations. The solid lines are for the pressure in the outer region set to zero ($\beta_2 = 0$), while the dashed line corresponds to zero core pressure ($\beta_1 = 0$).

have been identified. Agreement between $r_{\rm s,eff}$ and $r_{\rm s}$ is qualitatively good in the interval over which the plasma is unstable, and excellent near the interfaces. The $n = -16$ and $n = 9$ modes are near resonant with the outer and inner interfaces, respectively. As shown in figure 3(*a*), a stability scan with wall radius indicates that in the limit $r_{\rm w} \to 1$, modes for $n < 0$ are wall-stabilized. In the limit that the outer interface is made resonant with the $n = -16$ tearing mode (for example by changing R), $\Delta' \to \infty$. This mode is the current driven external kink of ideal MHD. Conversely, the unstable range for $n \geqslant 12$ is only very weakly affected by the wall position. If the inner interface is mode resonant with the perturbation, $\Delta' \to \infty$, and the mode is ideal unstable. This is the internal kink of ideal MHD.

Recently, Mills *et al* [6] demonstrated that one can unify ideal and relaxed variational treatments by extending the relationship between $\boldsymbol{b}$ and $\boldsymbol{\xi}$ through the Newcomb gauge $\boldsymbol{a} = \boldsymbol{\xi} \times \boldsymbol{B}$. If this variational treatment is followed, rational surfaces do explicitly enter the expression for ξ as derived from b_r, the variation in the radial part of the magnetic field, and so both relaxed and tearing modes become localized at the resonant surface r_s.

The findings of figure 2, obtained for a pressureless plasma, agree with that of Furth *et al* [15], who showed that for cylindrical pressureless plasma with no vacuum, Δ' is proportional to the second variation in the magnetic energy, which thus drives the tearing mode.

It is insightful to examine the influence of the Lagrange multiplier value on stability for variational and tearing mode treatments, and examine how stability relates to the q profile. For both variational and tearing mode treatment cases, if the edge Lagrange multiplier is changed to match the core, such that $\mu_1 = \mu_2 = 2.0$, q becomes everywhere positive: $q = 0.1$ at the core, drops to $q = 0.039$ at the plasma vacuum boundary, and then rises to $q = 0.469$ at the wall. In this case, there are no unstable $m = 1, n < 0$ modes, as there are no $q < 0$ resonant surfaces within the plasma. The plasma is however unstable to $m = 1, 17 \leqslant n \leqslant 25$ modes. Because there are no jumps in pressure or rotational transform at the interfaces, stability is insensitive to variation of the position of the interface. These results demonstrate that agreement between tearing mode and variational treatments is not contingent upon a special choice of Lagrange multiplier used. As expected, it is also a necessary but not sufficient condition that for a (m, n) tearing mode to be unstable, the corresponding resonant surface must be present in the plasma. As an aside, we remark that the stability conclusions for the $\mu_1 = \mu_2 = 2$ configuration investigated here differ from the Bessel function model of Gibson and Whiteman [16]. For $m = 1$ modes the Bessel function model is stable providing $\mu < 3.11$. The difference in treatments is the presence of a vacuum region, which is ignored in the Bessel function model, but retained here. In the limit that $r_{\rm w} \to 0$ in our work, the stability conclusions agree.

We have also compared stability conclusions drawn from variational and tearing mode treatments as a function of β. We find that while both variational and tearing mode treatments have the same stability trends with β, the marginal stability limit of the variational treatment (for a given m and n) is lower than that of tearing modes. A study is ongoing into the cause of this discrepancy, as well as formally relating $\delta^2 W$ to Δ'.

Finally, figure 3(*b*) is a plot of the marginal stability boundary ($\lambda = 0$) in $n - \beta$ space for $m = 1$ eigenmodes of the variational treatment. The two pressure profile configurations that have been studied are $\beta_1 = 0$ and $\beta_2 = 0$. Trends in the marginal stability boundary can be understood by relating the radial location of the mode resonant surface to the analogue of radial pressure gradient in the MRXMHD model: the sign and magnitude of nearby pressure jumps. For $n > 0$ modes resonant near the first interface, an increasing core pressure increases the pressure drop across the first interface, and so destabilizes the plasma. Conversely, increasing the edge pressure leads to a pressure jump across the first interface, and so stabilizes the internal modes. For $\beta_2 > 0.3$ all $m = 1$ internal modes ($n > 0$) are completely stabilized. For the $n < 0$ modes resonant near the edge, changes in the core pressure have little effect, while increasing the edge pressure destabilizes the plasma.

5. Conclusions

We have computed the stability MRXMHD plasmas using both a variational and a tearing mode treatment, evaluated in a periodic cylindrical configuration. The marginal stability conclusions of the two treatments for a zero β plasma, as well as the trends with β, appear to be identical, in agreement with earlier analytic working by Furth *et al* [15]. For such plasmas, we conclude that the space of allowed MRXMHD variations is identical to that of tearing modes plus ideal MHD modes. For nonzero β, some discrepancy exists between the marginal stability boundaries of variational and tearing mode treatments, with the stability limit of variational plasmas lower than that of tearing modes. A study is underway to resolve this discrepancy.

The overarching aim of this work has been to elucidate the nature of perturbations available to MRXMHD equilibria, which in turn is motivated by our quest for mathematically rigorous solutions of MHD force balance in 3D geometry. Our working extends the model of Tassi *et al* [8] to nonzero β multiple region relaxed plasmas that include a vacuum, and complements Mills *et al* [6], who demonstrated that that one can unify ideal and relaxed variational treatments through the Newcomb gauge. Combined, our results suggest that variational stability of MRXMHD configurations is sufficient for both ideal and tearing ($\Delta' < 0$) stability. This is to be expected because the MRXMHD constraints are a subset of the ideal MHD constraints, but allow reconnection. Consequently, the allowed variations of ideal MHD are a subset of MRXMHD [5]. The wider exploration of the space of allowed variations of MRXMHD is an area of ongoing research.

The relevance of stability studies of 2D configurations to the development of rigorous solutions of MHD force balance in 3D geometry is multi-fold. Recently, Mills *et al* [6] showed that configurations with a jump in rotational transform on either side of the barrier are internally unstable to ideal MHD modes. Hence, barriers can not support a jump in rotational transform. In earlier work [4] we identified that if the MRXMHD equilibrium is prescribed by plasma properties at specified interfaces, equation (5) becomes a nonlinear eigenvalue problem for the Lagrange multipliers, μ_i, with an infinite number of discrete solutions. Different solutions correspond to a different number of poles in the rotational transform [4]. However, as discussed in Taylor [17], the magnetic free energy increases with increasing μ, and so the higher eigenvalues are generally more unstable. In 3D we plan to use a descent algorithm to find a true minimum of the energy within a search space including multiple poloidal and toroidal Fourier harmonics, so that unstable solutions are automatically discarded. If there are multiple minima, algorithms for choosing the lowest energy minimum, for given constraints, will need to be used to find a nonlinearly stable solution.

In other ongoing work we are also exploring the maximum pressure jump an interface can support before it is destroyed by instabilities and chaos. We are also planning to improve the physical utility of the MRXMHD model, which at present is a minimal extension of ideal MHD equilibrium theory, being a zero-Larmor-radius, single-fluid, static model. We have in mind extending the model to comprise two fluids with flows, while remaining within a relaxation framework. A future plan is to explore the use of the double Beltrami model [18], which has been shown to be useful for describing the phenomenology of the pressure pedestal in H-mode tokamak discharges [19].

Acknowledgment

The authors would like to acknowledge the support of the Australian Research Council, through grant DP0452728.

References

[1] Hole M.J., Hudson S.R. and Dewar R.L. 2007 Equilibria and stability in partially relaxed plasma–vacuum systems *Nucl. Fusion* **47** 746–53

[2] Hole M.J., Hudson S.R. and Dewar R.L. 2006 Stepped pressure profile equilibria in cylindrical plasmas via partial taylor relaxation *J. Plasma Phys.* **77** 1167–71

[3] Kukushkin A.B. and Rantsev-Kartinov V.A. 1999 An extension of relaxed state principle to tokamak plasmas with ITBs *26th EPS Conf. on Controlled Fusion Plasma Physics (Maastricht, The Netherlands)* vol 23J pp 1737–40 http://epspdd.epfl.ch/Maas/web/pdf/p406.pdf

[4] Hudson S.R., Hole M.J. and Dewar R.L. 2007 Rotational-transform boundary value problem for beltrami fiels in toroidal domains *Phys. Plasmas* **14** 052505

[5] Dewar R.L., Hole M.J., McGann M., Mills R. and Hudson S.R. 2008 Relaxed plasma equilibria and entropy-related plasma self-organisation principles *Entropy* **10** 621–34

[6] Mills R., Hole M.J. and Dewar R.L. 2008 Magnetohydrodynamic stability of plasmas with ideal and relaxed regions *J. Plasma Phys.* (arXiv:0902.2612)

[7] Newcomb W.A. 1960 Hydromagnetic stability of a diffuse linear pinch *Ann. Phys.* **10** 232–67

[8] Tassi E., Hastie R.J. Porcelli F. 2007 Linear stability analysis of force-free equilibria close to taylor relaxed states *Phys. Plasmas* **14** 092109

[9] Martin P. *et al* and RFX mod team 2007 A new paradigm for RFP magnetic self-organization: results and challenges *Plasma Phys. Control. Fusion* **49** A177–93

[10] Kruskal M.D. and Kulsrud R.M. 1958 Equilibrium of a magnetically confined plasma in a toroid *Phys. Fluids* **1** 265–74

[11] Woltjer L. 1958 A theorem on force-free magnetic fields *Proc. Natl Acad. Sci.* **44** 489–91

[12] Taylor J.B. 1974 Relaxation of toroidal plasma and generation of reverse magnetic fields *Phys. Rev. Lett.* **33** 1139

[13] Chapman B.E., Almagri A.F., Anderson J.K. and Biewer T.M. 2002 High confinement plasmas in the Madison symmetric torus reverse-field pinch *Phys. Plasmas* **9** 2061–68

[14] Ortolani S. and the RFX team 2006 Active MHD control experiments in RFX-mod *Plasma Phys. Control. Fusion* **48** B371–81

[15] Furth H.P., Rutherford P.H. and Selberg H. 1973 Tearing mode in the cylindrical tokamak *Nucl. Fusion* **16** 1054–63

[16] Gibson R.D. and Whiteman K.J. 1968 Tearing mode instability in the Bessel function model *Plasma Phys.* **10** 1101–04

[17] Talyor J.B. 1986 Relaxation and magnetic reconnection in plasmas *Rev. Mod. Phys.* **58** 741–63

[18] Yoshida Z. and Mahajan S.M. 2002 Variational principles and self-organization in two-fluid plasmas *Phys. Rev. Lett.* **88** 095001

[19] Guzdar P.N., Mahajan S.M. and Yoshida Z. 2005 A theory for the pressure pedestal in high (H) mode tokamak discharges *Phys. Plasmas* **12** 032502